

## **Experimental Scale Model Study on Explosion of Clean Refrigerant Leaked in an Underground Plant Room**

Z.M Gao and Y. Gao  
College of Aerospace and Civil Engineering  
Harbin Engineering University  
Harbin, Heilongjiang, China

W.K. Chow\* and Y. Wan  
Research Centre for Fire Engineering  
Department of Building Services Engineering  
The Hong Kong Polytechnic University  
Hong Kong, China

C.L. Chow  
Department of Architecture and Civil Engineering  
City University of Hong Kong  
Hong Kong, China

\*Corresponding author:

Fax: (852) 2765 7198; Tel: (852) 2766 5843

Email: [beelize@polyu.edu.hk](mailto:beelize@polyu.edu.hk); [bewkchow@polyu.edu.hk](mailto:bewkchow@polyu.edu.hk)

Postal address: Department of Building Services Engineering, The Hong Kong Polytechnic University, Hung Hom, Kowloon, Hong Kong.

Submitted: March 2017

Revised: November 2017

Further revised: March 2018

## **Abstract**

Several clean refrigerants widely used in new air-conditioning systems are composed of flammable propane. Leakage of the flammable refrigerant from the air-conditioning systems housed in a basement plant room would pose fire and explosion hazards. However, very few studies have been carried out to study explosion hazards of leaked clean refrigerant in underground spaces. In this paper, a model chamber with two common mechanical ventilation designs in basement plant room was used to study experimentally the hazards. Clean flammable refrigerant was discharged to the model chamber to a concentration level less than the lower flammability limit. Four sets of tests with different ventilation conditions were carried. Concentrations of the leaked refrigerant at different positions in the chamber under different ventilation conditions were measured. Explosion of leaked gas was triggered by ignition. After ignition the transient gas temperature and pressure inside the model were recorded. Results indicate that mixing of leaked flammable refrigerant, and hence the concentrations of the leaked gas, depends on the mechanical ventilation design in the chamber. Improper ventilation provision would result in high refrigerant-to-air mixing ratio at some positions, even though the designed leaked refrigerant concentration is less than the lower flammable limit calculated from a well-mixing model. The results of the present study would contribute to better understanding of explosion hazards due to leakage of flammable refrigerant in green air-conditioning and refrigeration system in basement plant room or similar enclosures.

Keywords: explosion, clean refrigerants, air-conditioning and refrigeration system, ventilation

## **1. Introduction**

Mechanical plant rooms for air-conditioning and refrigeration systems are commonly allocated in underground basement spaces three levels below or even deeper under the ground level [1]. Currently, environmentally friendly green air-conditioning systems using propane refrigerant [2-5] are required by regulations in many countries. Propane refrigerant is flammable and may lead to accidental explosions [6-8]. Explosions resulting from leaked propane refrigerant have been reported [9-12] in Hong Kong since 2013. In densely populated urban areas such as Hong Kong, high quantities of combustibles are stored. Even the explosion of a small amount of propane refrigerant could be disastrous as observed in an accident before [9]. Explosion from leaked refrigerants can be much more hazardous in underground spaces as explosion control systems might not be installed. The gas pressure generated cannot be relieved to outside quickly because there are no openable windows or doors as in rooms above the ground. There is an urgent need to better understand [13-15] the explosion hazards of flammable refrigerants leaking from malfunctioning air-conditioning and refrigeration systems housed in underground spaces. With better understanding based on results of research, fire protection systems [1] with explosion control and appropriate suppressing agents can then be designed and specified.

Some studies on the ventilation design to disperse leaked flammable refrigerant were reported in the literature [16]. Experiments were carried out in a specially designed test facility to study the dispersion of leaked refrigerant using tracer gases such as carbon dioxide. From the measured tracer gas concentrations and observed flow patterns, the effects of parameters such as ventilation equipment and installation height of ventilation facility were studied. These results were used to draft guidance on the dispersion of flammable refrigerant in the event of

leakage. Design limits of ventilation parameters were also proposed [17]. A common guideline is that, even when flammable refrigerant leaks out, the lower flammable limit (LFL) should not be exceeded in the space concerned. Some authorities impose even more stringent guidelines requiring concentration not to exceed about one-fifth of LFL [15]. Explosion hazard in partially confined areas with very small amount of leaked gas has also been reported in a few studies [18,19].

Flammable refrigerants are usually heavier than air and possible to stay at lower level. However, mechanical ventilation with air intake from low level and exhaust at high level would bring gases up. In a room of size 3 m by 1.8 m by 3 m with refrigerant ‘850 R290’ leaking out from an air-conditioner, the average concentration can be up to 3%, falling within the LFL range (2.1%-9.5%). As refrigerant R290 is heavier than air, the concentration is distributed unevenly and can be ignited at positions with higher concentration. Therefore, studying the propane deflagration in the scaled room model will provide useful information on explosion hazards.

In addition to the overall allowable concentration (below the LFL) of leaked flammable refrigerant in a room, local flammable gas concentration is also important [20]. However, the mechanism and extent of mixing of flammable gas with air depends on the ventilation design. As propane is heavier than air, higher propane concentrations (above the LFL) is found at lower levels in a small flat when fresh air intake is at a higher level. Explosions might occur when there are small ignition sources and such incidents of explosion of flammable refrigerant have been reported [9]. The consequences of explosion in enclosed spaces, such as in underground spaces, can be very hazardous [21-24]. Better use of flammable refrigerants was raised recently [25-27].

In this paper, explosion of propane refrigerant leaking out from air-conditioning systems in a basement plant room was studied using scale models. The effects of the following two typical mechanical ventilation modes called 'extraction only' design [28,29] were studied with air inlets and outlets at high or low positions (Fig. 1):

- High level exhaust with fan and low level air intake without fan.
- Low level exhaust with fan and high level air intake without fan.

A model chamber was constructed with fixed amount of propane refrigerant injected. Possible explosion upon ignition was studied by measuring transient temperature and pressure distribution. Flame spread was observed. The experimental results and analysis are useful for better understanding the explosion hazards of leaked flammable refrigerants under these two ventilation modes by extraction in basement plant rooms housing air-conditioning and refrigeration systems.

## **2. Experimental Method**

The model room for experimental study on explosion hazards of leaked propane refrigerant is shown in Fig. 2(a). The model was of 1m length, 0.6 m width and 1m height, giving a floor area of 0.6 m<sup>2</sup> and space volume of 0.6 m<sup>3</sup> representing a 3m\*1.8m\*3m room. The mass of refrigerant is about 850 g in a normal air-conditioning unit. The corresponding gas injection mass of the scaled model room is 31.5 g (as shown in Table 1). The floor and walls of the model room were made of 2 mm thick stainless steel sheets. The ceiling of the room was made of 5 mm plexiglass sheet, so that the flame propagation process could be observed from the top.

An opening of area 0.04 m by 0.04 m was provided on the ceiling (12cm to the shorter edge and 28cm to the longer edge) and another on the side wall (12cm to the shorter edge and 28cm to the longer edge) of the room, for providing mechanical ventilation. The positions of the openings are shown in Fig. 2(a), with a photograph shown in Fig. 2(b).

Propane refrigerant was discharged from two copper tubes of diameter 6 mm, which were located near the center of the bottom of the room (Fig. 2(c)). The copper tube penetrated the floor of the model room, and then bent with outlets towards the floor. The distance of the two discharging points was 5 cm, and the height from the bottom was 10 cm. The propane refrigerant supply piping system is shown in Fig. 2(d). There is no other sealing with pressure relief from the vent.

A 200-g refrigerant bottle was used to inject 31.5 g of propane at a mass flow rate 2.69 g/min or a volumetric flow rate 1.5 litre/min. The filling up time was 720 s, giving an average concentration of propane of 3%. The exhaust vent area was  $0.2826 \times 10^{-4} \text{ m}^2$  or  $28.26 \text{ mm}^2$ .

The average exhaust speed was  $0.44 \text{ ms}^{-1}$ . Clean refrigerant R290 was used directly instead of tracer gas, because of the small chamber size. R290 is the common name for high purity (higher than 97.5%) propane ( $\text{C}_3\text{H}_8$ ) suitable for use in the refrigeration and air conditioning industry. The concentration of propane discharged into the chamber was adjusted to be common design figures calculated from 'well-mix' models [20]. The concentrations of the discharged propane at different positions were measured.

Two fans of identical models were mounted respectively on the top and side vents to provide different ventilation modes. According to the ventilation design standards, typical ventilation rates for restaurants are from 6 to 10 air changes per hour (ACH). The air volume required for

the fan was 6 to 10 m<sup>3</sup> / h. The exhaust fans used were capable of providing such a flow rate.

Propane concentration was measured using gas concentration sensor (MD61) with performance characteristics shown in Fig. 3. As specified in the manual, error range of the sensors for measuring gas concentration is 1.2% with working temperature from 0 °C to 40 °C. It can be seen from the figure that the sensor had a linear characteristic for many types of gases, including propane. The response recovery time is about 10 s. Because of its good linearity, the pure propane gas measuring voltage was calibrated for the 100% concentration.

A total of 12 0.2 mm K-type thermocouples were divided into 3 trees (T1 to T3) and placed at positions shown in Fig. 4(a). Each tree had 4 thermocouples TN1 to TN4 (N=1,2,3) placed at distances 5 cm, 20 cm, 50 cm, and 95 cm, respectively, above the ground.

Concentrations of propane were measured at a total of 13 points arranged in three levels shown in Fig. 4(b). The first level had 5 points C11, C12, C13, C14 and C15, at 5 cm above the floor. The second level had 2 points C21 and C22, at 15 cm above the floor. The third level had 3 points C31, C32 and C33, at 30 cm above the floor. Combustible gas concentration sensors of the heat conduction type were placed at the concentration measurement points. These concentration sensors could not stand high temperatures and had a long response time of 10 s to 30 s. Therefore, rapid concentration changes after combustion could not be detected. Two ventilating methods with different sealing were studied. Concentration distribution measurement was then carried out first. The gas was then ignited to study explosion.

There are three pressure measurement points labelled as P1 to P3 as shown in Fig. 4(c).

Pressure sensor CYB41 was chosen for measuring the pressure generated by explosion. The frequency response of the pressure sensor was 1000 Hz, measuring range 10 kPa and error range 0.1%. This gave a maximum error of  $\pm 10$  Pa in measuring pressure up to 1700 °C. This type of pressure sensor was suitable for installation on the walls of the model room only, but not within the room. The data acquisition system in conjunction with the pressure sensor was capable of simultaneous collection of up to 200 channels, with a maximum acquisition frequency of 100 Hz for a single channel.

Ignition was achieved using spark-ignition device located at the center of the room 20 cm above the floor (Fig. 4(d)).

A 120-frame high-definition camera was installed above the transparent ceiling of the model room (Fig. 4(e)) to take photographs of flame propagation.

Four tests with different ventilation conditions were carried out as shown in in Fig. 5.

- Test 1. Partially closed chamber without mechanical ventilation:  
Upper and lower vents having well defined small openings to simulate a plant room above the ground. Lower vent sealed when ignition.
- Test 2. Completely closed chamber without mechanical ventilation:  
Upper and lower vents closed, model sealed across boundaries of glass and metal frame by adhesives. This model arrangement is similar to an underground plant room without ventilation.
- Test 3. Mechanically ventilated chamber, mode 1:  
Extraction at upper vent, lower vent opened.



- Test 4. Mechanically ventilated chamber, mode 2:

Upper vent opened, extraction at lower vent.

After propane refrigerant had been injected into the chamber for 720 s, ignition was initiated.

The pressure and gas temperature at the measuring points were recorded. Flame spread patterns were also captured using the camera installed above the chamber.

A summary of measurements taken in the tests is given in Table 2.

As temperatures measured by thermocouples lag behind in rapid deflagration, it is difficult to get accurate transient temperature rises. This is another reason why temperature data in Test 2 was not measured. To reduce the response time delay, fine 0.2 mm wire was used with only 4 mm exposed to give faster response. The measured temperature will then be nearer to the actual value. Using cold end compensation and nonlinear correction with quadratic interpolation would measure temperature better. Cold end compensation would keep the cold end temperature rather constant to reduce fluctuations. Nonlinear correction method is used to solve nonlinear problems of thermocouples [30]. The above methods minimized the error caused by measuring dynamic response. The response time measured [30] by type K thermocouple was 10.3 ms with error range 1%, by using nonlinear correction method and cold end compensation. As deflagration lasted for about 7 s, this thermocouple arrangement is acceptable.

### **3. Results and Discussion**

#### **3.1 Concentration Distribution of Propane Refrigerant**

After injecting propane in Test 1, gas concentrations at the measurement points increased steadily with time as shown in Fig. 6(a). The 5 measuring points (C11, C12, C13, C14 and C15) on the first level at height 5 cm above the model room floor had the highest concentrations, with values up to 27%. At measurement point C15, the nearest to the injection point, the concentration increased very rapidly upon injecting propane. The rate of change decreased at the other measurement points on this level. The concentration at 700 s on the second level (C21 and C22) was about 15%. The concentration on the third level (C31, C32 and C33), which was 30 cm above the floor, was almost unchanged. As propane has a higher density than air, the gas stayed at the lower part (within 30 cm above the floor) of the chamber upon injection to the partially closed environment of Test 1.

Test 2 was carried out with the model room sealed completely. Thermocouple wires connection could not be put in. Transient gas temperatures and concentrations were not measured in this test.

In Test 3, owing to the exhaust fan at the ceiling to pull air out of the model room, the transient concentrations increased with slight fluctuation as shown in Fig. 6(b). Propane concentrations near to exhaust ports C11 and C14 were significantly lower than those at the other three points on the same level. The concentration at C22 (near the exhaust port) was also lower than that at C21. Propane concentrations near the floor (C11, C12, C13, C14) under this mode of ventilation were lower than the corresponding concentrations under the unventilated and partially closed condition in Test 1.

For Test 4 with extraction fan operated at lower level, the measured transient propane concentration (Fig. 6(c)) on the lowest level was slightly lower than the corresponding values

of Test 3 (upper exhaust ventilation). The maximum concentration was 19%, but the concentration on the second and third level was almost zero. The flammable propane stayed at regions below a height 15 cm above the floor under this ventilation condition with extraction fan operating. The gas concentration was less than the value of Test 3 with ventilation at the upper exhaust.

### **3.2 Gas Temperature and Pressure Distributions**

Transient temperature distributions for Tests 1, 3 and 4 are shown in Fig. 7. As observed, measurement points in Test 1 had both the highest temperature and the lowest temperature. Higher temperatures were recorded in Test 1 with more vigorous combustion. As the exhaust fan was operating at the upper vent in Test 3, the flammable gas stayed near to the floor of the model room. Large amount of flammable gas could not be discharged. Furthermore, flammable gas and air mixed better due to the fan-induced aerodynamics.

Air temperatures measured in Test 4 decreased faster than in the other two cases. The maximum temperature was about 250°C, with many measuring points having the temperatures close to this value. Judging from the temperature measured during combustion, drawing flammable gas near the room floor would give weaker burning.

From the temperature profile of each thermocouple tree for Test 1 in Fig. 8, points at 50 cm above the floor experienced the highest temperature, followed by the measuring points at 20 cm above the floor. The measuring point at the lower part of the model room had the highest concentrations but the lowest temperature. In comparing the temperature along the horizontal direction, position close to the vent on the T1 tree had the lowest temperature. Furthest away

from the vent T3 tree recorded the highest temperature.

Transient pressures for Tests 1 and 2 are plotted in Fig. 9. Pressure changes in Tests 3 and 4 were very small and not plotted.

As the chamber in Test 1 was not completely closed, pressure would be partially released on explosion. Only a small pressure change was recorded during the burning process as in Fig. 9(a). The pressure at measuring points P1 and P3 were slightly higher than that of P2. The period of pressure change lasted for about 7 s.

Sealing the two vents would give a completely enclosed chamber. Upon ignition of propane the pressure changed significantly within a very short period of time. The pressure rose to a maximum of 3 kPa for Test 2 (Fig. 9(b)), which was much higher than the pressure due to ignition with vents unsealed. Combustion lasted for about 3 s. Similar to Test 1, pressures recorded at P1 and P3 were slightly higher than that at P2.

Pressure measured at the P2 sensor rose to 50 Pa and then dropped to the atmospheric pressure. Incomplete combustion of R290 produced a large amount of soot after 15 s as shown in Fig. 10. Soot particles deposited at the pressure aperture of diameter 0.5 mm as in Fig. 10 would affect pressure measurement. Therefore, transient pressures were shown up to 15 s.

### 3.3 Flame Spread Patterns

The flame spread patterns upon ignition were observed from the top through the glass sheet. In Test 1 propane burnt vigorously upon ignition, with a fire ball as shown in the photographs in Fig. 11 (a). The flame spread out from the ignition point, which was 20 cm above the floor. Very vigorous flame burning was observed in the lower half of the chamber. The burning process lasted for about 5 s, with the chamber full of carbon residue.

The flame spread patterns in Test 3 and Test 4 are shown in Fig. 11(b) and (c). Burning was much more vigorous in Test 3 in which the exhaust fan was installed at the upper vent.

### 4. Theoretical Analysis

As shown in Fig. 8, the measured temperatures at different vertical and horizontal locations change obviously. To establish a single mathematical model, the dimensions of the physical problem are reduced to a certain range. Average temperatures at different positions and heights are predicted. A transient temperature equation was derived.

The following assumptions are made on the container and gas in developing the mathematical model:

- The deflagration process is short and no heat loss on the wall of the vessel;
- Heat loss from the wall after deflagration.
- The process from deflagration to discharge is regarded as isentropic. There is no loss of energy exchange between gases.

After ignition, the flame surface spreads rapidly to the periphery, the pressure inside the container increases and the temperature rises. When the flame propagates to the top of the vessel, the gas and air flow out and begin to release pressure. As deflagration is still going on and heat produced is higher than the heat loss, temperature rises at this time. Till deflagration ends, pressure decreases to a certain value, gas in the vessel does not flow out anymore and outside gas starts to enter the container. The pressure and temperature gradually revert to ambient pressure and room temperature. The whole process can be divided into 4 stages according to temperature and pressure change.

(1) Deflagration spread stage:  $0-t_1$ .

It starts from ignition ( $t=0$ ) and ends at flame spread to vessel top ( $t=t_1$ ). Propane combustion velocity is 0.4 m/s under atmospheric pressure. Distance of ignition point to vessel top is 0.8 m. Then, the flame surface spread time is 2.0 s. In this stage, temperature rises and pressure increases, no gas release from the gap.

As there is no gas release from the gap, gas mass remains unchanged.

$$m(t) = m_0 = \rho_0 V \quad (1)$$

$m_0$  is the quality of the original gas, and  $\rho_0$  is the density for the initial state.

The total energy of the gas in the vessel at the moment  $t$  is:

$$E(t) = m_0 C_{p0} T_0 + Q(t) \quad (2)$$

$C_{p0}$  is the initial specific heat at constant pressure and  $T_0$  is the initial temperature.

$$Q(t) = \frac{m_b(t)}{M} \Delta Q \quad (3)$$

$Q(t)$  is the heat emitted by propane that involved in combustion,  $m_b(t)$  is the propane

mass involved in combustion,  $M$  is the molecular weight of propane, and

$\Delta Q = 2200 \text{ KJ}/(\text{kg} \cdot \text{K})$  is propane combustion heat.

Gas temperature at  $t$ :

$$T(t) = \frac{E(t)}{m(t) C_p(t)} \quad (4)$$

where

$$C_p(t) = \frac{(m_0 - m_b(t)) C_{p0} + m_b(t) C_{pb}}{m_0} \quad (5)$$

is the specific heat capacity of mixed gas at constant pressure.

$C_{pb}$  is the specific heat of combustion product at constant pressure. Ignoring the variation of

specific heat at constant pressure with temperature.

$$T(t) = \frac{m_0 C_{p0} T_0 + \frac{m_b(t)}{M} \Delta Q}{(m_0 - m_b(t)) C_{p0} + m_b(t) C_{pb}} \quad (6)$$

(2) Gas release stage:  $t_1 - t_2$

Gas starts to release when flame surface spreads to the vessel top. As deflagration is still going on, heat produced is higher than the heat loss, temperature rises till  $t_2$ . Then, deflagration stops and temperature reaches the highest.

Combustion energy produces from  $t_1$  to  $t$ :

$$E_1(t) = \frac{m_b(t)}{M} \Delta Q \quad (7)$$

Gas release mass rate at  $t$ :

$$\dot{m}_2(t) = A \rho_2(t) V_2(t) \quad (8)$$

where  $A$  is gas release area,  $\rho_2(t)$  is gas release density and  $V_2(t)$  is gas release velocity.

Energy produces from  $t_1$  to  $t$ :

$$E_2(t) = \int_{t_1}^t \dot{m}_2(t) C_{p2}(t) T_2(t) dt = \int_{t_1}^t A \rho_2(t) V_2(t) C_{p2}(t) T_2(t) dt \quad (9)$$



Subscript 2 indicates parameters of the exhaust gas.

Gas mass in the vessel:

$$m(t) = m_0 - \int_{t-t_1}^t m_2(t)dt = m_0 - \int_{t-t_1}^t A\rho_2(t)V_2(t)dt \quad (10)$$

Ignoring heat transfer loss, temperature at t is:

$$T(t) = \frac{E(t_1) + E_1(t) - E_2(t)}{m(t)C_p(t)} = \frac{E(t_1) + \frac{m_b(t)}{M}\Delta Q - \int_{t_1}^t A\rho_2(t)V_2(t)C_{p2}(t)T_2(t)dt}{(m_0 - \int_{t-t_1}^t A\rho_2(t)V_2(t)dt)C_p(t)} \quad (11)$$

(3) Gas intake stage:  $t_2 - t_3$

As deflagration ends, inner gas pressure is lower than atmospheric pressure, ambient air enters the vessel. When pressure is restored to atmospheric pressure, it is marked as  $t_3$ .

Indraft gas mass rate at t:

$$\dot{m}_3(t) = A\rho_3(t)V_3(t) \quad (12)$$

Subscript 3 indicates parameters of the indraft gas.

The total energy of the system increases:

$$E_3(t) = \int_{t_1}^t \dot{m}_3(t) C_{p3}(t) T_3(t) dt = \int_{t_1}^t A \rho_3(t) V_3(t) C_{p3}(t) T_3(t) dt \quad (13)$$

The total energy of the system:

$$m(t) = m_0 - \int_{t-t_1}^t m_2(t) dt = m(t_2) + \int_{t-t_2}^t A \rho_3(t) V_3(t) dt \quad (14)$$

The mixture gas temperature at t:

$$T(t) = \frac{E(t_2) + E_3(t)}{m(t) C_p(t)} = \frac{E(t_2) + \int_{t_2}^t A \rho_3(t) V_3(t) C_{p3}(t) T_3(t) dt}{(m(t_2) + \int_{t-t_2}^t A \rho_3(t) V_3(t) dt) C_p(t)} \quad (15)$$

(4) Heat dissipation stage:  $t_3 - t_4$

When the pressure inside the container is restored to atmospheric pressure, the quality of the gas in the container does not change anymore. The system energy exchange with atmosphere depends on the heat convection. The temperature curve ends at  $t_4$ .

Gas mass in the container at t:

$$m(t) = m(t_3) \quad (16)$$

Energy releasing out the system:

$$\dot{e}_4(t) = qS_A = h(T(t) - T_0)S_A \quad (17)$$

where  $q$  is heat flux density,  $S_A$  is heat conduction area,  $T_0$  is ambient air temperature and  $h$  is convective heat transfer coefficient.

Mixture gas temperature at  $t$ :

$$T(t) = \frac{E(t_3) - E_4(t)}{m(t)C_p(t)} = \frac{E(t_3) - \int_{t_3}^t h(T(t) - T_0)S_A dt}{m(t_3)C_p(t)} \quad (18)$$

The calculation formula of temperature in the container is:

$$T(t) = \begin{cases} \frac{m_0 C_{p0} T_0 + \frac{m_b(t)}{M} \Delta Q}{(m_0 - m_b(t))C_{p0} + m_b(t)C_{pb}}, & 0 < t \leq t_1 \\ \frac{E(t_1) + \frac{m_b(t)}{M} \Delta Q - \int_{t_1}^t A \rho_2(t) V_2(t) C_{p2}(t) T_2(t) dt}{(m_0 - \int_{t_1}^t A \rho_2(t) V_2(t) dt) C_p(t)}, & t_1 < t \leq t_2 \\ \frac{E(t_2) + \int_{t_2}^t A \rho_3(t) V_3(t) C_{p3}(t) T_3(t) dt}{(m(t_2) + \int_{t_2}^t A \rho_3(t) V_3(t) dt) C_p(t)}, & t_2 < t \leq t_3 \\ \frac{E(t_3) - \int_{t_3}^t h(T(t) - T_0) S_A dt}{m(t_3) C_p(t)}, & t_3 < t \leq t_4 \end{cases} \quad (19)$$

The ignition time is 0, according to propane combustion velocity  $t_1 = 2.0$  s, The temperature still rises and pressure reaches the maximum, agreeing with stage 1.

With the exhaust process going on, the pressure in the container decreases gradually and the

pressure curve reaches the lowest at  $t_2 = 6$  s.

When air intake process begins, the pressure in the container increases and restores to atmospheric pressure at  $t_3 = 9.0$  s, Stage III ends.

According to the time domain of the temperature curve,  $t_4 = 45.0$  s.

Initial parameters are shown in Table 3.

Stage I:

$$m(t) = 1.1558t, \quad T(t) = \frac{246.57 + 77.79t}{0.83} \quad (20)$$

Stage II:

$m_b(t) = 16.8(t - t_1)$  Exhaust gas flow rate is considered constant  $\rho_2 V_2 A = 0.085 \text{ kg/s}$ . The specific heat at constant pressure and temperature of exhaust gas are considered constant (same with  $t_1$ ).

$$C_{p2}(t)T_2 = 1.031 * (163.17 + 273.15) = 449.85 \quad (21)$$

Before  $t = 4$  s, deflagration continues,

$$T(t) = \frac{362.14 + 16.8(t - t_1) - 0.085 * 449.85 * (t - t_1)}{(0.805 - 0.085(t - t_1)) * 1.031} \quad (22)$$

After  $t = 4$  s, deflagration ends,

$$m_b(t) = 16.8(t - t_1), \quad \rho_2 V_2 A = 0.085 \quad (23)$$

$$C_{p2}(t)T_2 = 1.031 * (214.5 + 273.15) = 502.77 \quad (24)$$

$$T(t) = \frac{362.14 + 16.8 * 2 - 0.085 * 502.77 * (t - t_1)}{(0.805 - 0.085(t - t_1)) * 1.031} \quad (25)$$

Stage III:

$$\text{In Stage II, } m(t_2) = 0.635\text{kg}, \quad E(t_2) = 306.9\text{KJ} \quad (26)$$

Taking  $\rho_3 V_3 A = 0.05$

$$C_{p3}(t)T_3 = 1.004 * 297.22 = 298.4 \quad (27)$$

$$T(t) = \frac{306.9 + 0.05 * 298.4 * (t - t_2)}{(0.635 + 0.05 * (t - t_2)) * 1.031} \quad (28)$$

Stage IV:

$$m(t_3) = 0.885\text{kg}, \quad E(t_3) = 381.5\text{KJ} \quad (29)$$

In order to avoid solving the differential equation, the average temperature at Stage IV is used as the high temperature of convection heat transfer, and ambient air temperature as the low temperature.

$$\overline{T(t)} = \frac{149.86 + 76.26}{2} + 273.15 = 386.21\text{K} \quad (30)$$

$$T(t) = \frac{381.5 - 5.62/1000 * (386.21 - 297.22) * 3.8 * (t - t_3)}{0.885 * 1.031} \quad (31)$$

Experimental and theoretical temperature curves are shown in Fig. 12.

## 5. Conclusions

Experiments on explosion of leaked propane refrigerant in a model chamber under different ventilation conditions were performed. Flammable gas concentrations before ignition and transient temperatures and pressures after ignition were measured. The following conclusions can be drawn from the present study:

- The pressure rise for igniting flammable refrigerant in the partially closed chamber in Test 1 was not very high, with a maximum value below 500 Pa. However, the leaked refrigerant burned vigorously to give a fireball with high gas temperature at that instance. This test simulates the scenario of a room above ground level in a building.
- Ignited propane refrigerant in the closed chamber in Test 2 would give a very high pressure of 3 kPa in the model. This test simulates the scenario of an unventilated basement plant room.
- With the exhaust fan installed at the upper vent (Test 3) the burning process was very vigorous, with much higher gas temperatures recorded in the chamber than in Test 4. This test simulates one common design mode of mechanical ventilation.

- With extraction at a lower level (Test 4) the burning process was not so vigorous as in the case with extraction at higher level (Test 3) because this mode of extraction would take more flammable gas out of the chamber. This test simulates another mode of mechanical ventilation.
- In view of the higher density of propane refrigerant than air, mechanical ventilation with extraction at a lower level is more efficient in removing propane in case of leakage.
- In all the cases, the transient gas temperature during burning was very high at positions near to the middle part of the chamber at a height about 0.5 m above the floor, lying within the occupied zone. This is very hazardous to occupants and firefighters at the occupied zone in a real room. Thus leakage of propane refrigerant in a plant room could be very hazardous.

## **Funding**

The work described in this paper was supported by a grant from the Research Grants Council of the Hong Kong Special Administrative Region for the project “A study on explosion hazards of clean refrigerant propane leaking from air-conditioning units in small commercial flats” (PolyU 152034/14E) with account number B-Q42U.

## References

1. Codes of Practice for Minimum Fire Service Installations and Equipment and Inspection Testing and Maintenance of Installation and Equipment, Fire Services Department, Hong Kong Special Administration Region (2012).
2. E. Granryd, "Hydrocarbons as refrigerants – An overview", *International Journal of Refrigeration*, Vol. 24, pp. 15-24 (2001).
3. Philip C.H. Yu and W.K. Chow, "Zero-ODP impact on building sustainability", *Proceedings of SASBE 2006 - 2<sup>nd</sup> CIB International Conference on Smart and Sustainable Built Environments*, Shanghai, China, 15-17 November 2006, p. 302-309 (2006).
4. E. Baskin, N.D. Smith, R. Perry and M. Tufts, "Flame suppression and lubricant interaction of hydrocarbon mixtures for household refrigerator/freezers", 1994 *International CFC and Halon Alternatives Conference: Stratospheric Ozone Protection for the 90's: Conference Proceedings*, October 24-26, 1994, Washington, D.C., pp. 32-37.
5. J.M. Calm, "The next generation of refrigerants – Historical review, considerations, and outlook", *International Journal of Refrigeration*, Vol. 31, pp. 1123-1133 (2008).
6. H. Lunde and G. Lorentzen, "Accidents and critical situations due to unintentional escape of refrigerants: a survey of cases in Norway over the last two decades", *International Journal of Refrigeration*, Vol. 17, pp. 371-373 (1994).
7. I.L. Maclaine-cross, "Usage and risk of hydrocarbon refrigerants in motor cars for Australia and the United States", *International Journal of Refrigeration*, Vol. 27, pp. 339-345 (2004).
8. "HyChill gas in NZ coolstore fatality", *Climate Control News*, p. 6, August 2008.
9. The Standard, "21 hurt in lunch blast", Hong Kong, 10 January 2013.



10. W.K. Chow, “Lesson learnt from a recent incident in Ma On Shan : Any explosion risk for environmentally friendly refrigerants?”, Department of Building Services Engineering, The Hong Kong Polytechnic University, Hong Kong, February 2013.  
Available at:  
[http://www.bse.polyu.edu.hk/researchCentre/Fire\\_Engineering/Hot\\_Issues.html](http://www.bse.polyu.edu.hk/researchCentre/Fire_Engineering/Hot_Issues.html).
11. South China Morning Post, “Seven injured in Ap Lei Chau apartment blaze”, Hong Kong, 14 April 2013.
12. Ming Pao Daily News, “Two hurt in refrigerated truck explosion”, Hong Kong, p. A04, 5 March 2013 – In Chinese.
13. Y.W. Ng and W.K. Chow, “Fire hazards of refrigerants in air conditioning system”, 15<sup>th</sup> International Refrigeration and Air Conditioning Conference, 14-17 July 2014, Purdue, West Lafayette, USA.
14. Y.W. Ng and W.K. Chow, “Use of clean refrigerants and their potential fire hazards in Hong Kong”, ASME-ATI-UIT 2015 Conference on Thermal Energy Systems: Production, Storage, Utilization and the Environment, 17-20 May 2015, Napoli, Italy.
15. Y.W. Ng and W.K. Chow, “Fire safety precautions for heating, ventilation, air conditioning and refrigeration equipment/systems using environmentally friendly refrigerants”, The 10<sup>th</sup> International Green Energy Conference, 24-27 May 2015, Taichung, Taiwan.
16. D. Colbourne and K.O. Suen, “Equipment design and installation features to disperse refrigerant releases in rooms – Part I: experiments and analysis”, International Journal of Refrigeration, Vol. 26, No. 6, pp. 667-673 (2003).
17. D. Colbourne and K.O. Suen, “Equipment design and installation features to disperse refrigerant releases in rooms – Part II: determination of procedures”, International Journal of Refrigeration, Vol. 26, No. 6, pp. 674-680 (2003).

18. Y.D. Jo and J.Y. Kim, "Explosion hazard analysis in partially confined area", Korean Journal of Chemical Engineering, Vol. 18, No. 3, pp. 292-296 (2001).
19. R.A. Ogle, "Explosion hazard analysis for an enclosure partially filled with a flammable gas", Process Safety Progress, Vol. 18, No. 3, pp. 170-177 (1999).
20. W.K. Chow, "On ventilation design for underground car parks", Tunnelling and Underground Space Technology, Vol. 10, No. 2, p. 225-246 (1995).
21. Hanifi Copur, Muammer Cinar, Gunduz Okten and Nuh Bilgin, "A case study on the methane explosion in the excavation chamber of an EPB-TBM and lessons learnt including some recent accidents", Tunnelling and Underground Space Technology, Vol. 27, p. 159-167 (2012).
22. J.C. Li, H.B. Li, G.W. Mab and Y.X. Zhou, "Assessment of underground tunnel stability to adjacent tunnel explosion", Tunnelling and Underground Space Technology, Vol. 35, p. 227-234 (2013).
23. V.R. Feldgun, Y.S. Karinski and D.Z. Yankelevsky, "The effect of an explosion in a tunnel on a neighboring buried structure", Tunnelling and Underground Space Technology, Vol. 44, p. 42-55 (2014).
24. Behnam Mobaraki and Mohammad Vaghefi, "Numerical study of the depth and cross-sectional shape of tunnel under surface explosion", Tunnelling and Underground Space Technology, Vol. 47, p. 114-122 (2015).
25. S. Kujak, "Flammability and new refrigerant options", ASHRAE Journal, May 2017, pp. 16-24.
26. W.K. Chow, Y.W. Ng and T.K. Yue, "Flammability and new refrigerant options", ASHRAE Journal, Letter to the Editor, December 2017, p. 9.
27. National Fire Protection Association, "Fire fighter flammable refrigerants training: Hazard assessment and demonstrative tests", Request for Proposals for Project

Contractor, NFPA Research Foundation, 27 February 2018.

28. W.K. Chow, “Any explosion risk for environmentally friendly refrigerants?”, Invited talk, Chemical Safety Seminar organized by Occupational Safety and Health Council, Hong Kong Convention and Exhibition Center, 22 March 2016.
29. W.K. Chow and Y.W. Ng, “Fire and explosion hazards of clean refrigerants”, Green Cross, Vol. 26 No. 3, p. 25-27 (2016) – In Chinese.
30. P. Lv, D. Pei and D. Shen, “The research of transient thermometry technology based on k-style thermocouple”, Chinese Journal of Sensors and Actuators. Vol. 27, p.775-780 (2014).

TUST\_SMExpCRA17-2a

**List of tables:**

Table 1: Refrigerant injection mass

Table 2: Summary of measurements in tests

Table 3. Initial parameters

**List of figures:**

Fig. 1: Two common mechanical ventilation modes

Fig. 2: Experimental setup

Fig. 3: Performance characteristics of gas concentration sensor MD61

Fig. 4: Measurement points layout

Fig. 5: Four tests with different ventilation conditions

Fig. 6: Transient refrigerant concentration

Fig. 7: Transient gas temperature

Fig. 8: Gas temperature measured at each thermocouple tree for Test 1

Fig. 9: Transient gas pressure in Tests 1 and 2

Fig. 10. Thick soot due to incomplete combustion

Fig. 11: Flame patterns in Test 1, Test 3 and 4

Fig. 12. Experimental and theoretical average temperature

**Table 1. Refrigerant injection mass**

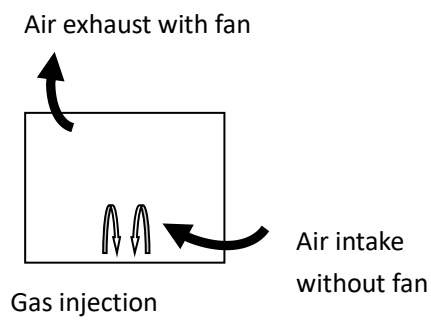
	Volume(m <sup>3</sup> )	Leakage mass(g)	Concentration	LFL×V(g)
Room	3×1.8×3=16.2	850	3%	615.6
Scaled model room	1×0.6×1=0.6	31.5	3%	22.8

**Table 2. Summary of measurements in tests**

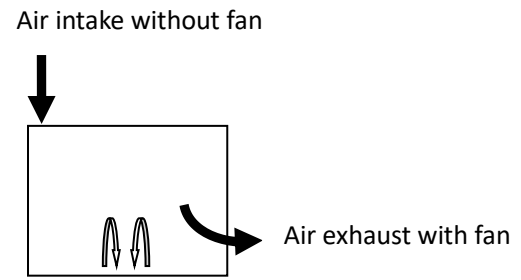
	Propane conc.	Gas temperature	Pressure	Flame pattern
Test 1	✓	✓	✓	✓
Test 2			✓	
Test 3	✓	✓		✓
Test 4	✓	✓		✓

**Table 3. Initial parameters**

Initial temperature	Air density	Vessel heat exchange area	Natural convection heat transfer coefficient
K	kg/m <sup>3</sup>	m <sup>2</sup>	
297.22	1.29	3.8	5.62



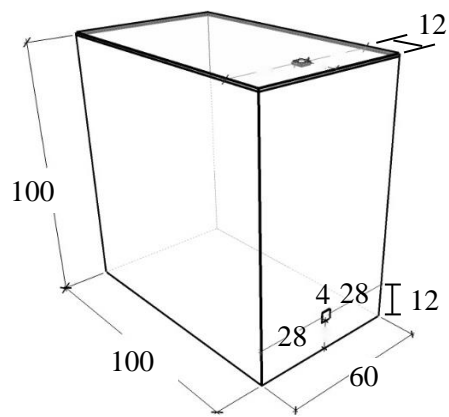
(a) High level exhaust with fan and low level intake without fan



(b) Low level exhaust with fan and high level intake without fan

**Fig. 1. Two common mechanical ventilation modes**



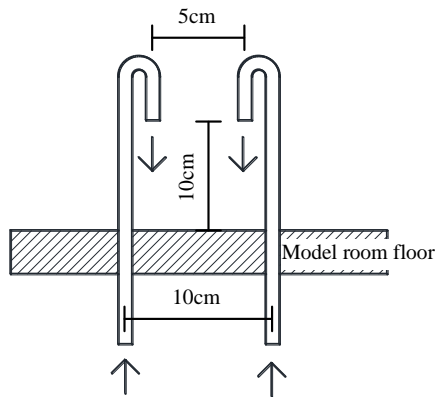


Dimensions in cm

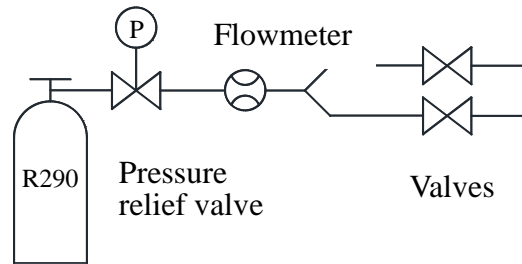
(a) The model room



(b) Photograph of the model room



(c) Layout of the fuel leaking points



(d) Supply system of refrigerant

**Fig. 2. Experimental setup**

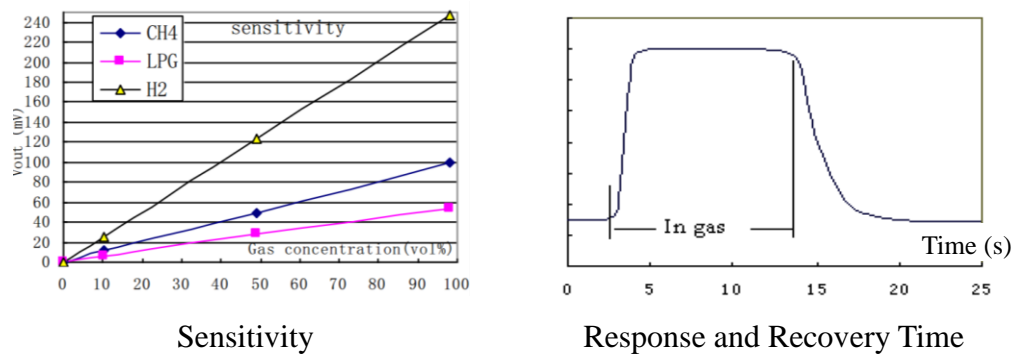
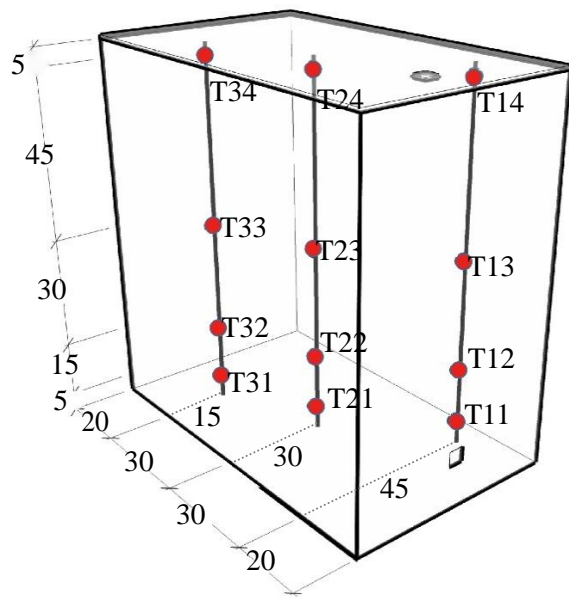
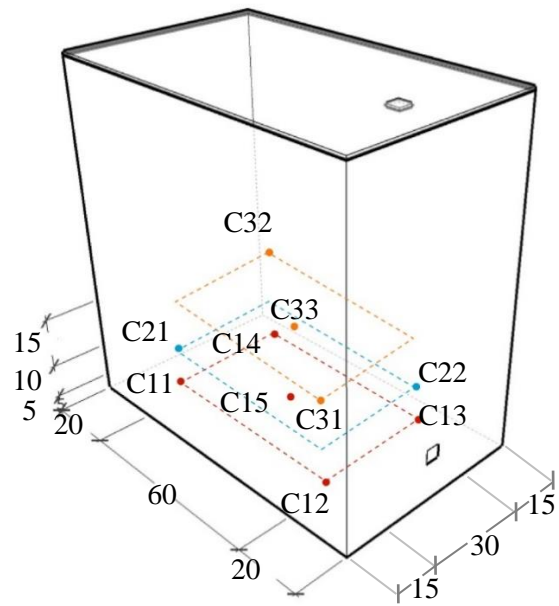


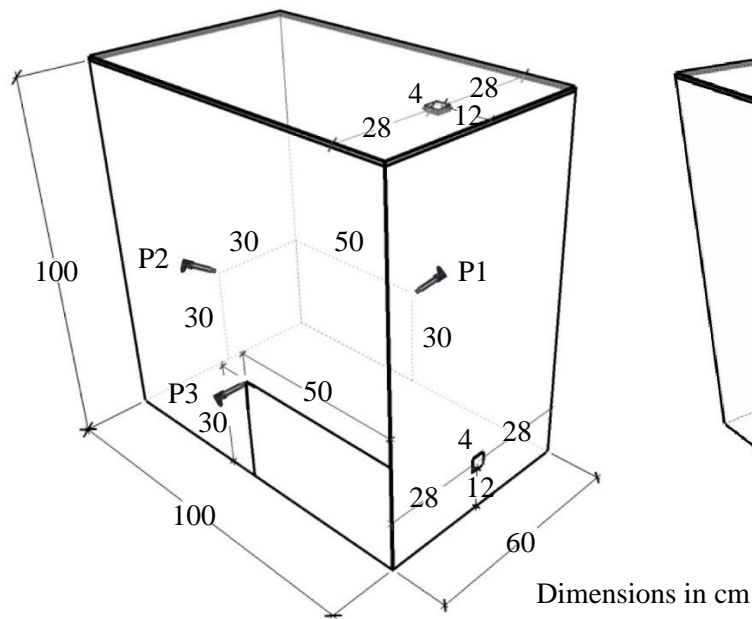
**Fig. 3. Performance characteristics of gas concentration sensor MD61**



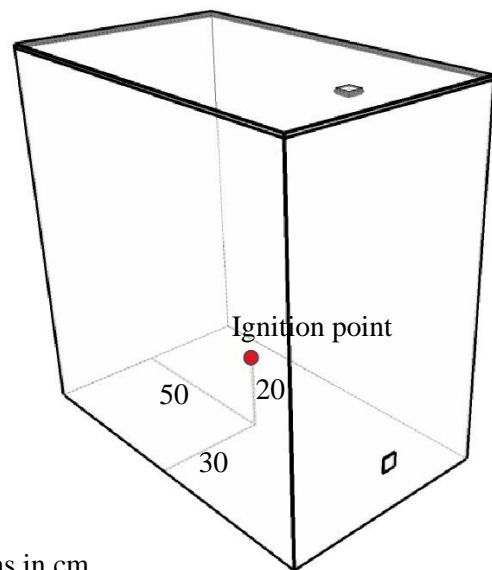
(a) Gas temperature



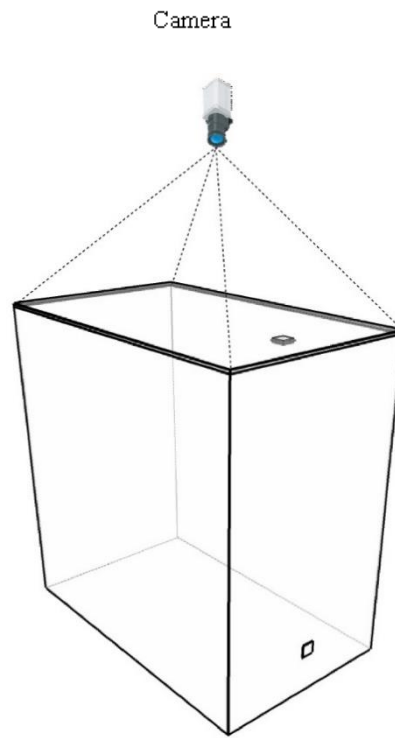
(b) Refrigerant concentration



(c) Pressure



(d) Ignition position



(e) Camera position

**Fig. 4. Measurement points layout**

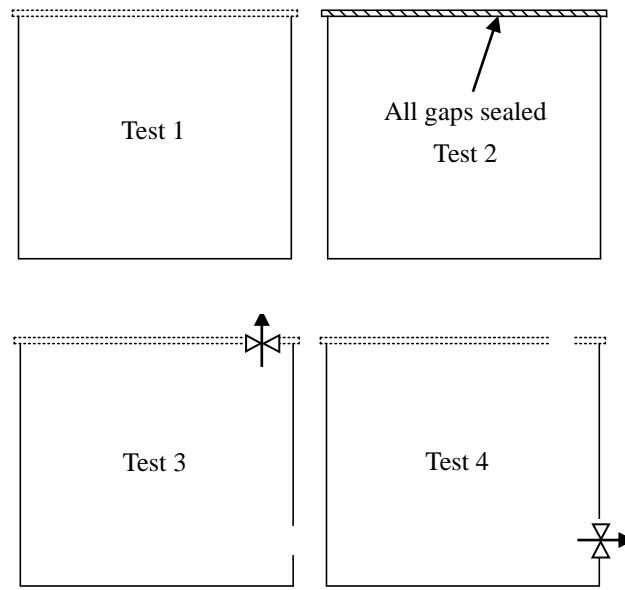
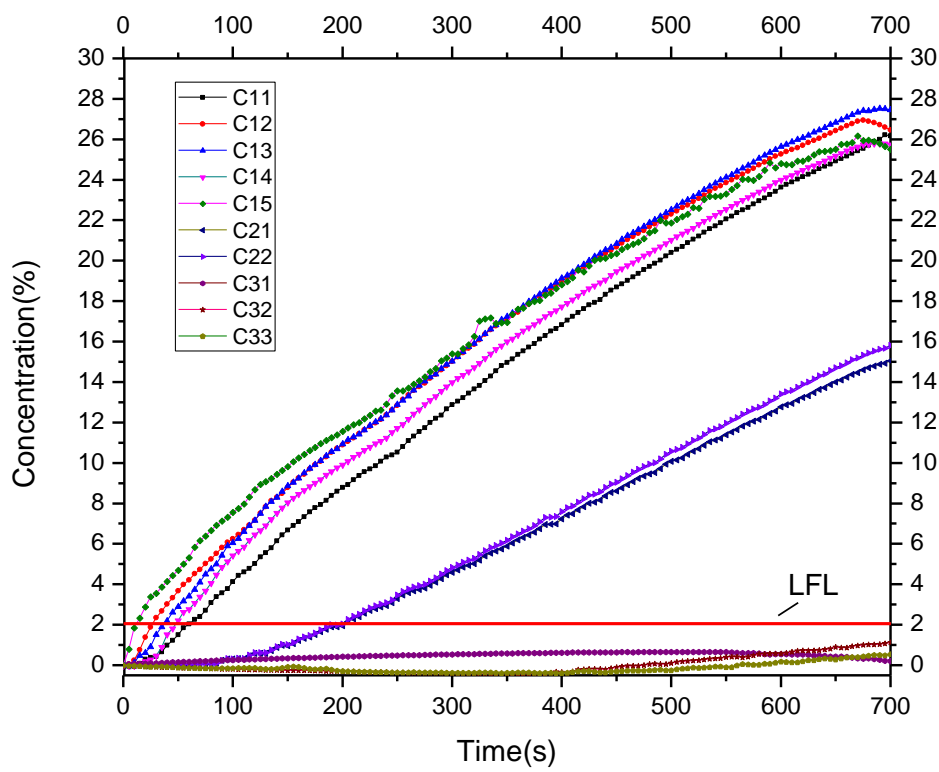
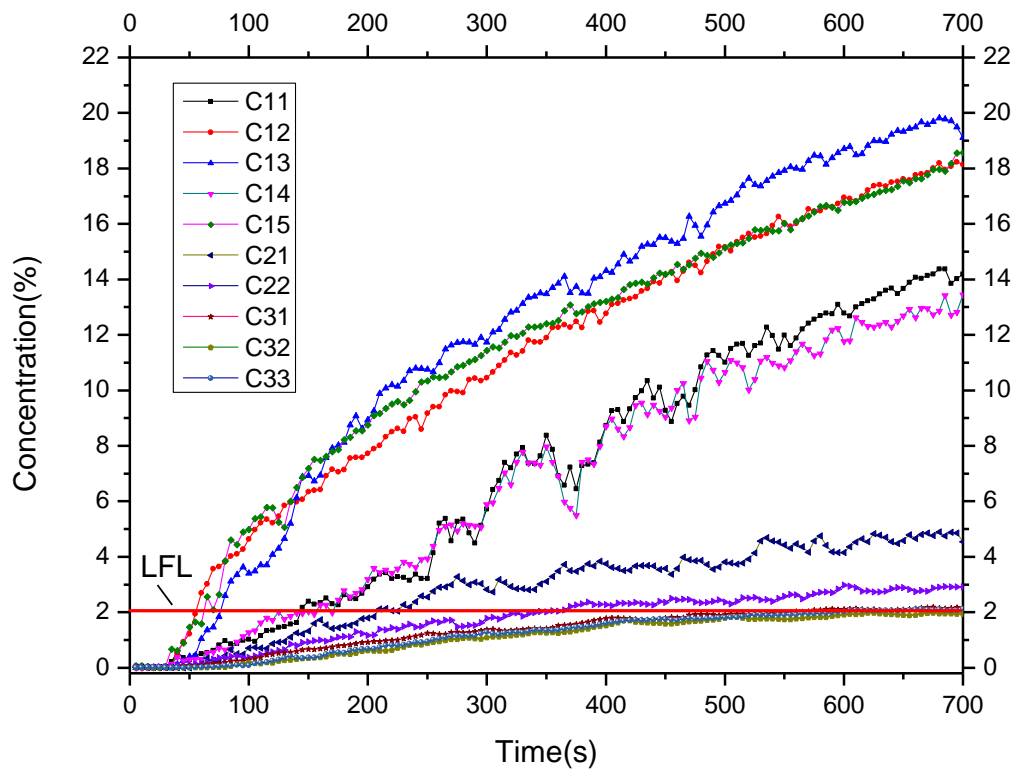


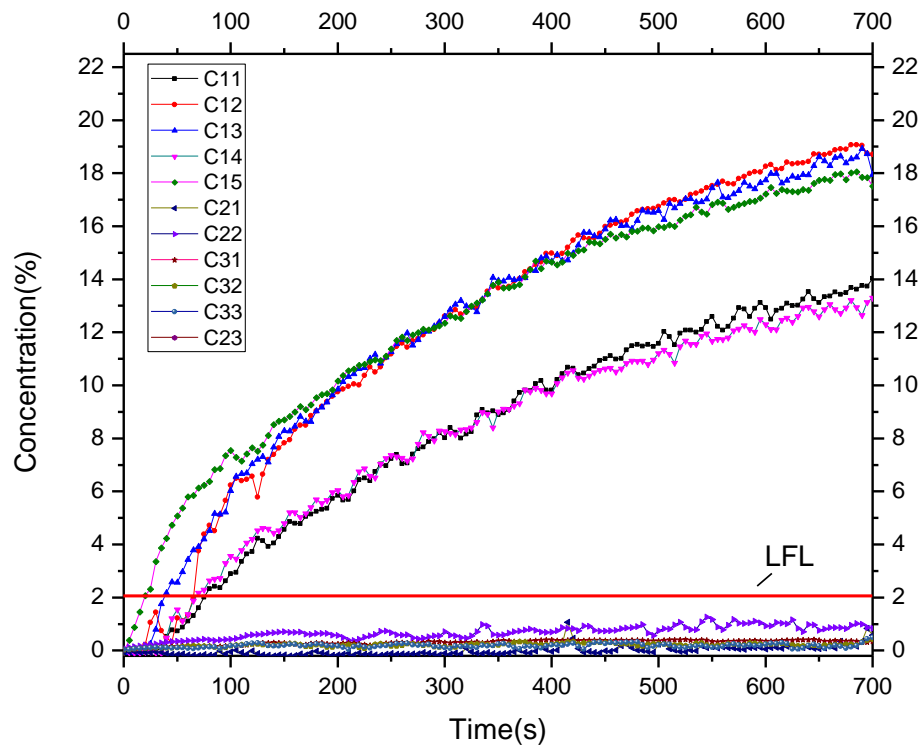
**Fig. 5. Four tests with different ventilation conditions**



(a) Test 1

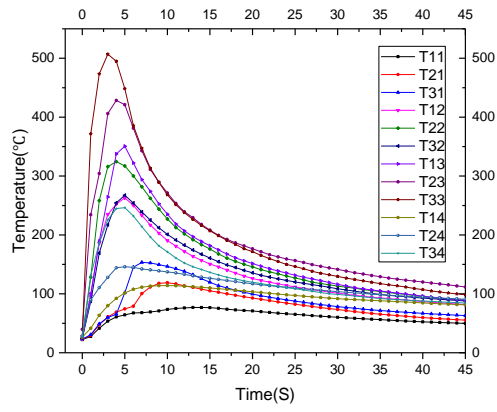


(b) Test 3

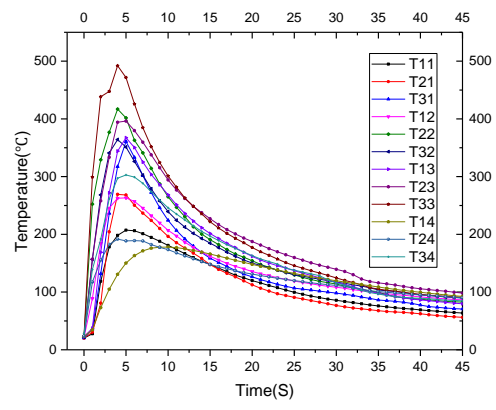


(c) Test 4

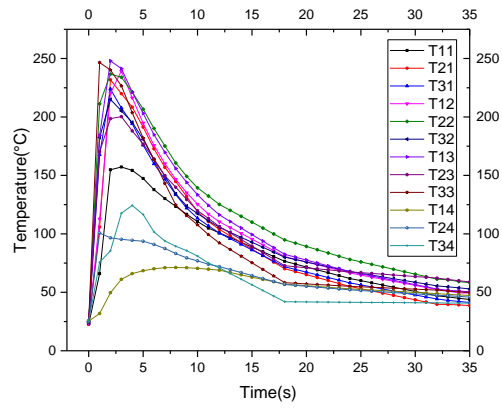
**Fig. 6. Transient refrigerant concentration**



(a) Test 1



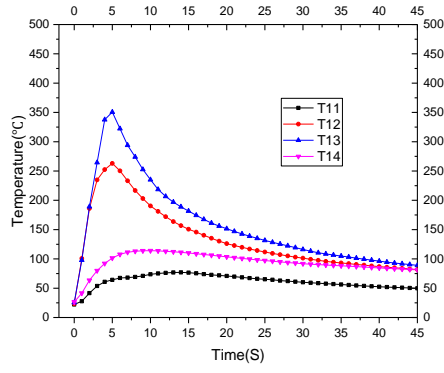
(b) Test 3



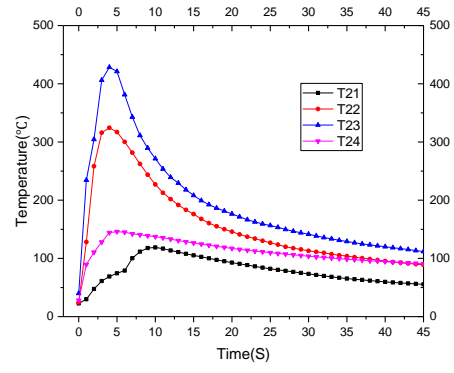
(c) Test 4

**Fig. 7. Transient gas temperature**

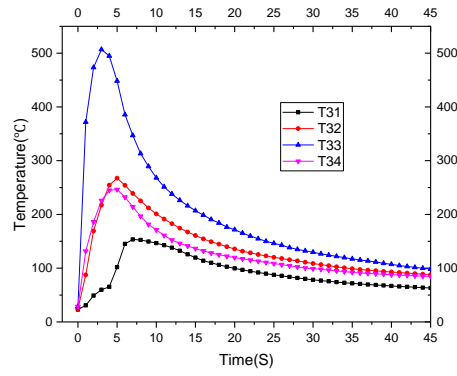




(a) T1

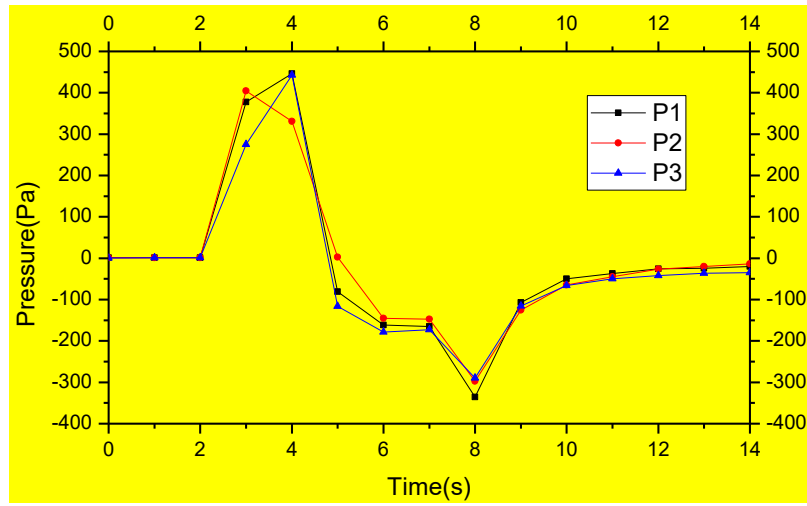


(b) T2

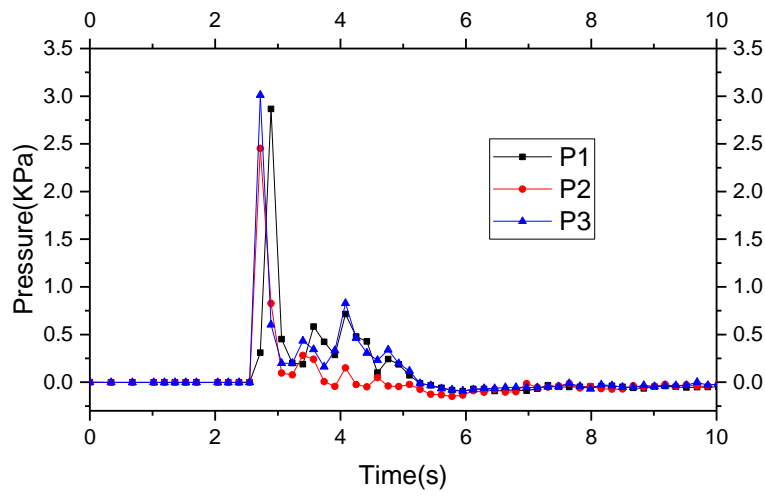


(c) T3

**Fig. 8. Gas temperature measured at each thermocouple tree for Test 1**



(a) Test 1



(b) Test 2

**Fig. 9. Transient gas pressure in Tests 1 and 2**



**Fig. 10. Thick soot due to incomplete combustion**

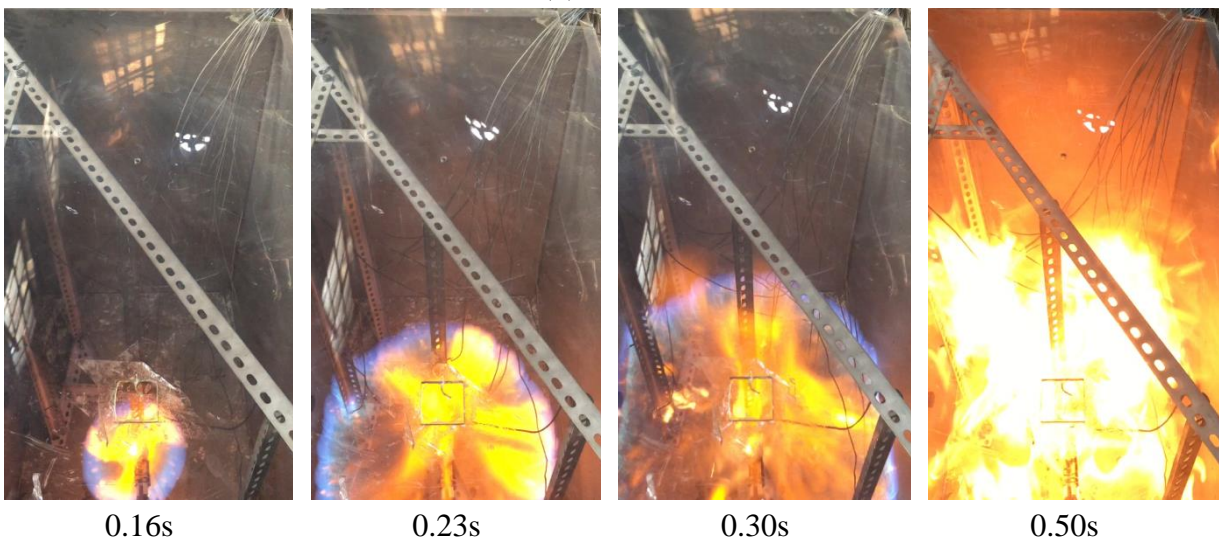
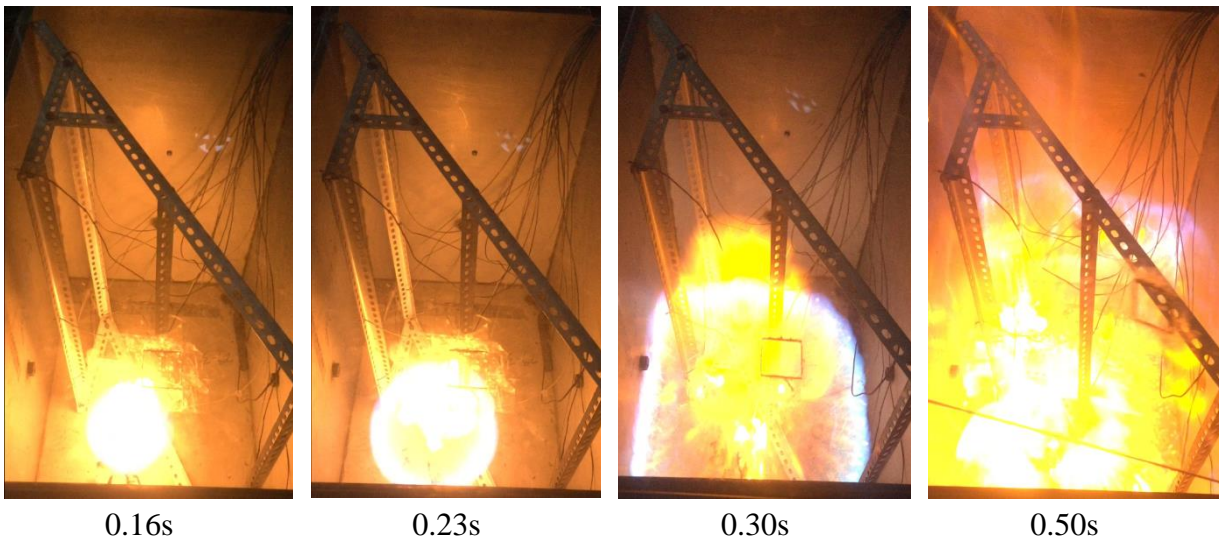
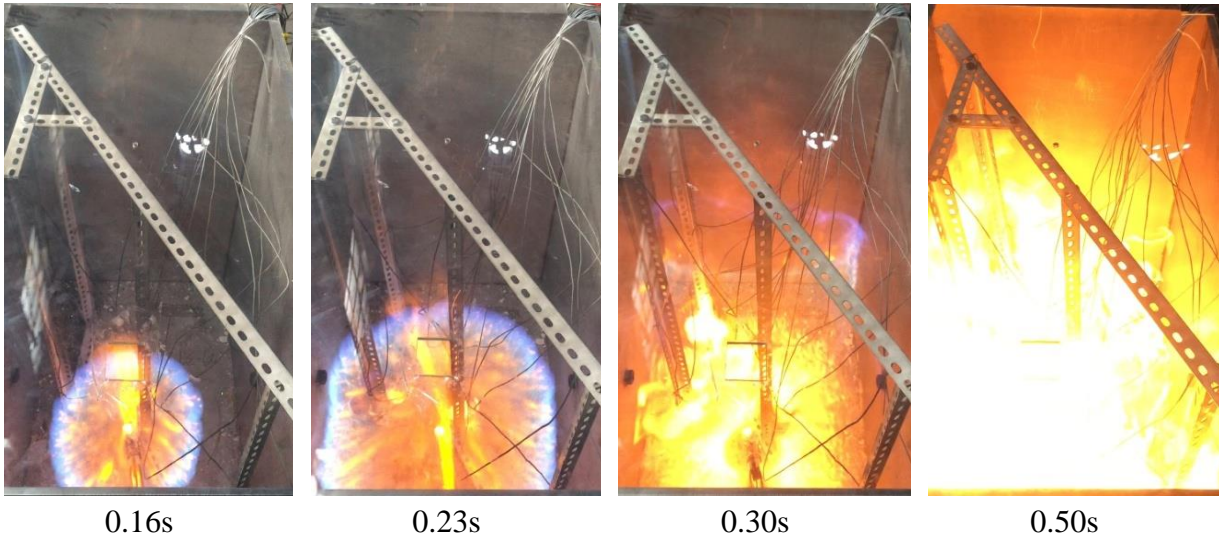


**Fig. 11.** Flame patterns in Test 1, Test 3 and 4

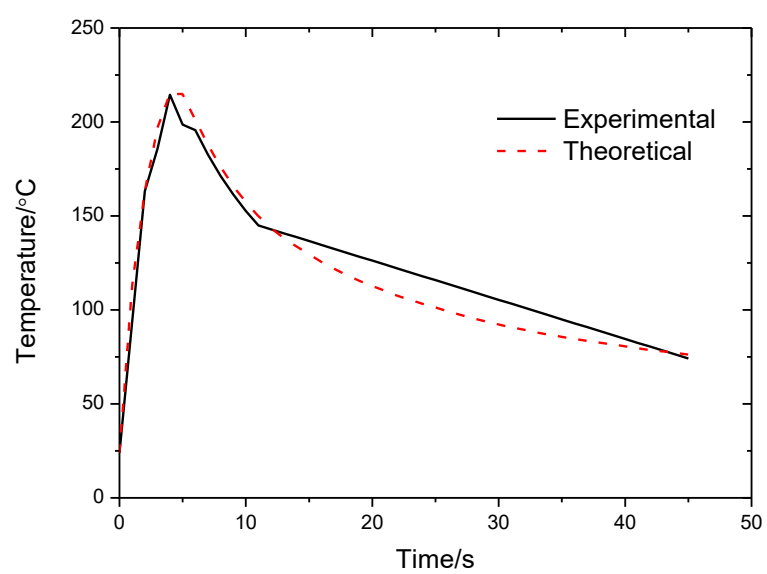


**Fig. 12.** Experimental and theoretical average temperature